Atmos. Chem. Phys., 14, 11185–11199, 2014
www.atmos-chem-phys.net/14/11185/2014/
doi:10.5194/acp-14-11185-2014

Atmospheric Chemistry and Physics Open Access

Re-evaluating the reactive uptake of HOBr in the troposphere with implications for the marine boundary layer and volcanic plumes

T. J. Roberts[1], L. Jourdain[1], P. T. Griffiths[2], and M. Pirre[1]

[1]LPC2E, UMR 7328, CNRS-Université d'Orléans, 3A Avenue de la Recherche Scientifique, 45071 Orleans, CEDEX 2, France
[2]Centre for Atmospheric Science, Cambridge University, Chemistry Department, Lensfield Road, Cambridge, CB2 1EW, UK

Correspondence to: T. J. Roberts (tjardaroberts@gmail.com)

Received: 15 November 2013 – Published in Atmos. Chem. Phys. Discuss.: 27 January 2014
Revised: 3 June 2014 – Accepted: 12 August 2014 – Published: 23 October 2014

Abstract. The reactive uptake of HOBr onto halogen-rich aerosols promotes conversion of $Br^-_{(aq)}$ into gaseous reactive bromine (incl. BrO) with impacts on tropospheric oxidants and mercury deposition. However, experimental data quantifying HOBr reactive uptake on tropospheric aerosols is limited, and reported values vary in magnitude. This study introduces a new evaluation of HOBr reactive uptake coefficients in the context of the general acid-assisted mechanism. We emphasise that the termolecular kinetic approach assumed in numerical model studies of tropospheric reactive bromine chemistry to date is strictly only valid for a specific pH range and, according to the general acid-assisted mechanism for HOBr, the reaction kinetics becomes bimolecular and independent of pH at high acidity.

This study reconciles for the first time the different reactive uptake coefficients reported from laboratory experiments. The re-evaluation confirms HOBr reactive uptake is rapid on moderately acidified sea-salt aerosol (and slow on alkaline aerosol), but predicts very low reactive uptake coefficients on highly acidified submicron particles. This is due to acid-saturated kinetics combined with low halide concentrations induced by both acid-displacement reactions and the dilution effects of $H_2SO_{4(aq)}$. A mechanism is thereby proposed for reported Br enhancement (relative to Na) in H_2SO_4-rich submicron particles in the marine environment. Further, the fact that HOBr reactive uptake on H_2SO_4-acidified supra-micron particles is driven by $HOBr+Br^-$ (rather than $HOBr+Cl^-$) indicates self-limitation via decreasing γ_{HOBr} once aerosol Br^- is converted into reactive bromine.

First predictions of HOBr reactive uptake on sulfate particles in halogen-rich volcanic plumes are also presented. High (accommodation limited) $HOBr+Br^-$ uptake coefficient in concentrated ($> 1\ \mu mol\ mol^{-1}\ SO_2$) plume environments supports potential for rapid BrO formation in plumes throughout the troposphere. However, reduced HOBr reactive uptake may reduce the rate of BrO cycling in dilute plumes in the lower troposphere.

In summary, our re-evaluation of HOBr kinetics provides a new framework for the interpretation of experimental data and suggests that the reactive uptake of HOBr on H_2SO_4-acidified particles is substantially overestimated in current numerical models of BrO chemistry in the troposphere.

1 Introduction

The reactive uptake of HOBr onto halogen-containing aerosols to release Br_2 enables propagation of the chain reaction leading to autocatalytic BrO formation, the so-called "bromine explosion" (Vogt et al., 1996), first proposed following the discovery of ozone depletion events in the polar boundary layer (Barrie et al., 1988). Rapid and substantial (tens of ppbv) ozone depletion occurs upon the formation of just tens of pptv BrO due to cycling between Br and BrO, with further Br-mediated impacts on environmental mercury in the conversion of Hg^0 to more reactive and easily deposited form Hg^{II} (Schroeder et al., 1998). Tropospheric BrO chemistry has since been recognised outside the polar regions, with BrO identified above salt pans (Hebestreit et al., 1999), in the marine boundary layer (Read et al., 2008),

and is suggested to have a significant impact on the chemistry of the free troposphere (e.g. von Glasow et al., 2004). In particular, recent evidence of rapid BrO formation in acidic volcanic plumes (tens of pptv to ppbv on a timescale of minutes) has highlighted volcanic halogen emissions as a source of reactive bromine entering the troposphere (Bobrowski et al., 2003):

$$HOBr_{(g)} \rightarrow HOBr_{(aq)} \quad (R1)$$

$$HOBr_{(}aq) + Br^-_{(aq)} + H^+_{(aq)} \rightarrow Br_2(aq) + H_2O_{(l)} \quad (R2)$$

$$HOBr_{(aq)} + Cl^-_{(aq)} + H^+_{(aq)} \rightarrow BrCl_{(aq)} + H_2O_{(l)} \quad (R3)$$

$$BrCl_{(aq)} + Br^-_{(aq)} \leftrightarrow Br_2Cl^-_{(aq)} \quad (R4)$$

$$\leftrightarrow Br_2(aq) + Cl^-_{(aq)} Br_2(aq) \rightarrow Br_2(g) \quad (R5)$$

$$Br_2(g) \xrightarrow{h\nu} 2Br_{(g)} \quad (R6)$$

$$2Br_{(g)} + 2O_3(g) \rightarrow 2BrO_{(g)} + 2O_2(g) \quad (R7)$$

$$2BrO_{(g)} + 2HO_2(g) \rightarrow 2HOBr_{(g)} + 2O_2(g). \quad (R8)$$

Key to reactive halogen formation is the cycle of Reactions (R1)–(R8) which results in autocatalytic formation of BrO. Accommodation of $HOBr_{(g)}$ to aerosol Reaction (R1), followed by reaction with $Br^-_{(aq)}$ or $Cl^-_{(aq)}$ and $H^+_{(aq)}$ results in a dihalogen product (Reactions R2, R3). The reaction of HOBr with $Cl^-_{(aq)}$ (Reaction R3) is typically considered the dominant reaction pathway (albeit an assumption that may not apply in highly acidified aerosol as we show in this study) given that sea-salt aerosol contains $[Br^-_{(aq)}] \ll [Cl^-_{(aq)}]$ by a factor of 700 (or greater once reactive bromine formation has commenced), and the termolecular rate constants for Reactions (R2) and (R3) are of comparable magnitudes (Liu and Margarem, 2001; Beckwith et al., 1996). However, Br_2 is commonly the observed product, as confirmed by laboratory experiments by Fickert et al. (1999). The product conversion from BrCl to Br_2 is explained by aqueous-phase equilibria (Reaction R4) that interconvert BrCl into Br_2 (via Br_2Cl^-) before gaseous release (Reaction R5). According to equilibrium constants reported by Wang et al. (1994), conversion of BrCl to Br_2 is favoured at room temperature in aerosol provided $Br^-_{(aq)}$:$Cl^-_{(aq)} > \sim 10^{-4}$, as for example in sea-salt aerosol where $Br^-_{(aq)} : Cl^-_{(aq)} \approx 1.5 \times 10^{-3}$. The dihalogen species then partition into the gas phase, Reaction (R5). The exsolution of dihalogens from the aerosol to the gas phase also limits the occurrence of reverse reactions that might reform HOBr. Once in the gas phase, Br_2 is photolysed to produce 2 Br radicals, Reaction (R6), which may react with ozone to form BrO, Reaction (R7). HOBr is reformed via the reaction of BrO with HO_2, Reaction (R8), whereupon it may react again with halogen-containing aerosol to further propagate the cycle, each time doubling the concentration of reactive bromine.

Numerical models have been developed to better understand the formation of BrO and evaluate impacts on atmospheric oxidants throughout the troposphere and on mercury cycling in the environment. Models capture the salient features of BrO formation and impacts (e.g. on ozone depletion and Hg deposition events) in the different tropospheric environments (see reviews by Simpson et al., 2007 and Saiz-Lopez and von Glasow, 2012). Nevertheless, a number of uncertainties remain. For example, models tend to overestimate Br_x cycling in the marine environment (Sander et al., 2003; Smoydzin and von Glasow, 2007; Keene et al., 2009). Models predict a depletion in the inorganic bromine content of all acidified marine aerosols, as a consequence of HOBr reactive uptake to form Br_2 and its release into the gas phase. However, an aerosol bromine deficit is only observed in the slightly acidified supra-micron fraction, whilst aerosol bromine is found to be enhanced (relative to that expected based on Br : Na ratios in sea salt, using sodium as a sea-salt tracer) in the highly acidified sub-micrometre fraction. This phenomenon has not been explained to date (Sander et al., 2003). Numerical models have also attempted to simulate reactive halogen chemistry in volcanic plume environments. Models initialised with a high-temperature source region are able to reproduce the rapid formation of BrO in the near-source plume (Bobrowski et al., 2007; Roberts et al., 2009; von Glasow, 2010), as well as ozone depletion (Kelly et al., 2013), but a source of model uncertainty is the representation of heterogeneous halogen chemistry on volcanic aerosol, which may differ from that reported from experiments on sea-salt aerosol.

All these studies rely on laboratory experiments to quantify rate constants of the reactions, with a key process in the formation of reactive bromine being the reaction of $HOBr_{(aq)}$ with halide ion $X^-_{(aq)}$ ($Cl^-_{(aq)}$ or $Br^-_{(aq)}$) and $H^+_{(aq)}$, Reactions (R2, R3), which can be written generically as

$$HOBr_{(aq)} + H^+_{(aq)} + X^-_{(aq)} \xrightarrow{k_{ter}, k^{II}, k^{I}} BrX_{(aq)} + H_2O_{(aq)} \quad (R9)$$

Experimental studies (e.g. Fickert et al., 1999) show that the reaction of $HOBr_{(aq)}$ is promoted when alkaline sea-salt aerosol becomes acidified, either by natural (e.g. methane sulfonic acid) or anthropogenic (e.g. sulfuric acid) sources of acidity. However, laboratory experiments have reported uptake coefficients on acidified sea-salt aerosol, > 0.2 (Abbatt and Wachewsky, 1998) and 10^{-2} (Pratte and Rossi, 2006), a discrepancy that has not been explained to date. In addition, no experiments have been performed to quantify the uptake of HOBr on volcanic aerosol under tropospheric conditions.

Numerical model studies of reactive bromine chemistry currently implement Reaction (R9) using three-body reaction kinetics, i.e. it is assumed that the reaction rate is directly proportional to $H^+_{(aq)}$ concentration (e.g. von Glasow, 2002), or using uptake coefficients calculated on this assumption (see Ammann et al., 2013 and the IUPAC Task group evaluation website, 1999–present). We highlight, however, that earlier literature on the general acid-assisted mechanism for this and similar reactions (e.g. Eigen and Kustin, 1962;

Nagy et al., 1988) identify that the pH dependence of the reaction rate is more complex, with acid saturation of the kinetics at high acidity.

This study re-evaluates HOBr reactive uptake in the context of the general acid-assisted mechanism for the first time. The plan of the paper is as follows. In Section 2 the method for calculating the reactive uptake coefficient is recalled and the approach based on the general acid-assisted mechanism is explained. The data used to evaluate the new uptake coefficient calculations are presented. In Sect. 3 pH-dependent second-order rate constants (k^{II}) are derived for both HOBr+Br^- and HOBr+Cl^- in the context of the general assisted mechanism, using reported literature data for the underlying rate constants, and a thermodynamic model to predict aerosol composition under experimental conditions. Using the new parameterisation for k^{II}, reactive uptake coefficients for HOBr+Br^- and HOBr+Cl^- are calculated and compared to reported laboratory data for HCl-acidified sea-salt aerosol (Abbatt and Wachewsky, 1998) and H_2SO_4-acidified sea-salt aerosol (Pratte and Rossi, 2006). We provide new quantification of HOBr+Br^- and HOBr+Cl^- uptake coefficients on H_2SO_4-acidified sea-salt aerosol in the marine environment, and sulfuric acid aerosol in volcanic plumes dispersing into the troposphere. In Sect. 4, reactive uptake coefficients are calculated for HOBr on H_2SO_4-acidified sea-salt aerosol in the marine environment, and on sulfuric acid aerosol in volcanic plumes entering the troposphere, and implications discussed for BrO chemistry in these environments.

2 Method and experimental data

2.1 Quantifying the reactive uptake coefficient, γ_{HOBr}

The reactive uptake of $HOBr_{(g)}$ can be quantified by Eq. (1) (with further modification required for large particles due to the limitation of gas-phase diffusion) in terms of the reactive uptake coefficient, γ_{HOBr}, where v_{HOBr} is the mean molecular velocity of $HOBr_{(g)}$, cm s^{-1}, and Area is the surface area density of the aqueous phase, $cm^2\ cm^{-3}$.

γ_{HOBr} is a fractional number that quantifies the likelihood of reaction given a collision of $HOBr_{(g)}$ with a particle, and can be calculated following the resistor-model framework (Eq. 2) that describes the accommodation to the aerosol, and the reaction and diffusion in or across the aerosol particle. γ_{HOBr} is a function of several parameters, including accommodation coefficient, α_{HOBr}, the solubility of HOBr, H^*, the aqueous-phase diffusion rate, D_l, the gas constant R, Temperature, T, the mean molecular velocity, v_{HOBr}, and the first-order rate constant for the reaction of $HOBr_{(aq)}$, k^I. The parameter l is a function of D_l and k^I, $l = (D_l/k^I)^{0.5}$:

$$-\frac{\mathrm{d}[HOBr_{(g)}]}{\mathrm{d}t} = \gamma_{HOBr} \cdot \frac{v_{HOBr}}{4} \cdot [HOBr_{(g)}] \cdot \mathrm{Area} \quad (1)$$

$$\frac{1}{\gamma_{HOBr}} = \frac{1}{\alpha_{HOBr}} + \frac{v_{HOBr}}{4 \cdot H^*_{HOBr} \cdot R \cdot T \cdot \sqrt{D_{l,HOBr} \cdot k^I}} \cdot \frac{1}{\coth\left[\frac{r}{l}\right] - \frac{l}{r}} \quad (2)$$

$$-\frac{\mathrm{d}[HOBr_{(aq)}]}{\mathrm{d}t} = k^I \cdot [HOBr_{(aq)}] \quad (3)$$

$$k^I = k_{ter} \cdot [X^-_{(aq)}] \cdot [H^+_{(aq)}] \quad (4)$$

$$k^I = k^{II} \cdot [X^-_{(aq)}]. \quad (5)$$

To date, numerical models have adopted two approaches to simulate the reactive uptake of HOBr. Detailed process models (e.g. MISTRA; von Glasow et al., 2002; MECCA; Sander et al., 2011) tend to model HOBr gas–aerosol partitioning to and from the aerosol directly, with the reaction of HOBr inside the aerosol simulated using Eq. (3) and termolecular kinetics (Eq. 4). On the other hand, global models (e.g. in studies by von Glasow et al., 2004; Yang et al., 2005; Breider et al., 2010; Parella et al., 2012) tend to simulate HOBr reactive uptake as one step, Eq. (1), quantified by the uptake coefficient, γ_{HOBr}. The IUPAC evaluation recommends uptake coefficient to be calculated using Eq. (2) and the termolecular approach to HOBr kinetics, Eq. (4). In global models, a fixed uptake coefficient, γ_{HOBr}, is typically used for computational reasons.

However, as we highlight in this study, the termolecular kinetics approach (Eq. 4) is only valid within a limited pH range. Here we instead use Eq. (2) and the reaction kinetics of $HOBr_{(aq)}$ in terms of a second-order rate constant, Eq. (5), where k^{II} is a variable function of pH according to the general acid-assisted reaction mechanism for HOY+X^-(+H^+) constrained by available laboratory data. Details on the mechanism and derivation of k^{II} are given in Sect. S1 of the Supplement and Sect. 3.1). Despite being well documented (Eigen and Kustin, 1962; Kumar and Margarem, 1987; Nagy et al., 1988; Gerritsen and Margarem, 1990; Wang and Margarem, 1994), this mechanism has not been implemented in any numerical model studies of reactive halogen chemistry to date.

To calculate reactive uptake coefficients (Eq. 2), we also need to determine the aerosol composition, specifically halide concentration, $[X^-_{(aq)}]$ and the acidity. Indeed, $[X^-_{(aq)}]$ is needed for Eq. (5) and subsequently Eq. (2), and the acidity is also needed to determine k^{II} in the context of the general assisted mechanism (see the expression in Sect. 3.1) and subsequently Eqs. (5) and (2). This was achieved using the E-AIM (extended aerosol inorganic model, Carslaw et al., 1995; Clegg et al., 1998; Wexler and Clegg, 2002) and Henry's constants, (Sander, 1999, for more details see Sect. S3 of the Supplement). Given the high ionic strength of the solutions studied, concentrations were converted to activities using activity coefficients provided by E-AIM.

Finally, we assume in Eq. (2) an accommodation coefficient of 0.6 (Wachsmuth et al., 2002), with solubility and diffusion coefficients for HOBr in water and sulfuric acid derived from Frenzel et al. (1998), Iraci et al. (2005) and Klassen et al. (1998). A radius of 0.1 or 1 μm was assumed, reflecting the presence of both sub- and supra-micron particles in volcanic and marine environments. Further details are provided in Sect. S2 of the Supplement.

We compare our new approach to reported estimates of HOBr reactive uptake coefficients from laboratory experiments as outlined below.

2.2 Reported experimental studies on the reactive uptake of HOBr onto liquid aerosol

A number of laboratory experiments (Table 1) have quantified the reactive uptake of HOBr onto acidified sea-salt aerosol under tropospheric conditions (as well as on solid particles, not considered here). The accommodation coefficient for HOBr onto supersaturated $NaBr_{(aq)}$ aerosol was determined by Wachsumth et al. (2002) to be $\alpha_{HOBr} = 0.6 \pm 0.2$ at 298 K.

Experiments using acidified sea-salt particles made by nebulising a 5 M NaCl and 0.5 M HCl solution under conditions representative of the troposphere found the reactive uptake coefficient for the reaction ($HOBr+Cl^-$) to be very high ($\gamma_{HOBr} > 0.2$) on deliquesced aerosol (RH > 75 %, $T = 298$ K), (Abbatt and Waschewsky, 1998). Conversely, experiments by Pratte and Rossi (2006) on H_2SO_4-acidified sea-salt aerosol with H_2SO_4 : NaCl molar ratio = 1.45 : 1 at 296 K measured a substantially lower HOBr uptake coefficient, $\gamma_{HOBr} \sim 10^{-2}$, with a dependence on relative humidity ($\gamma_{HOBr} \sim 10^{-3}$ below 70 % RH). This large (10^1–10^2) discrepancy has not been resolved to date. Uptake of HOBr on pure sulfate aerosol at 296 K is found to be low ($\gamma_{HOBr} \sim 10^{-3}$), Pratte and Rossi (2006).

Aqueous-phase rate constants for the reaction of $HOBr+X^-+H^+$ have also been reported: for $HOBr+Br^-_{(aq)}$, Eigen and Kustin (1962) and Beckwith et al. (1996) report termolecular rate constants of $k_{ter} = 1.6 \times 10^{10}\,M^{-2}\,s^{-2}$ over a pH range of 2.7–3.6 and 1.9–2.4 at 298 K, respectively. For $HOBr+Cl\text{-}_{(aq)}$, Liu and Margarem (2001) report a three-body rate constant of $2.3 \times 10^{10}\,M^{-2}\,s^{-2}$ in buffered aerosol at pH = 6.4 and 298 K. Pratte and Rossi (2006) derived first-order rate constants for the reaction of $HOBr_{(aq)}$ from their uptake experiments, finding $k^I \sim 10^3\,s^{-1}$.

The IUPAC subcommittee for gas kinetic data evaluation currently recommends an uptake coefficient parameterisation utilising accommodation coefficient $\alpha_{HOBr} = 0.6$ (Wachsmuth et al., 2002), and first-order rate constant $k^I = k_{ter} \cdot [H^+_{(aq)}] \cdot [X^-_{(aq)}]$, with $k_{ter} = 2.3 \times 10^{10}\,M^{-2}\,s^{-1}$ (Liu and Margarem, 2001) for $HOBr+Cl^-$ and $k_{ter} = 1.6 \times 10^{10}\,M^{-2}\,s^{-1}$ (Beckwith et al., 1996) for $HOBr+Br^-$. Assuming a $Cl^-_{(aq)}$ concentration of 5.3 M typical of seawater and low uptake coefficients in alkaline sea-salt aerosol (Ammann et al., 2013 and the IUPAC evaluation website, 1999–present), this parameterisation yields a high uptake coefficient, $\gamma_{HOBr} \sim 0.6$, on acidified sea-salt aerosol, and is in agreement with $\gamma_{HOBr} \geq 0.2$ reported by Abbatt and Waschewsky (1998) while overestimating the uptake coefficient as reported by Pratte and Rossi (2006) by a factor of ~ 20.

Here we present new uptake calculations based on the general acid-assisted mechanism rather than termolecular kinetics in an attempt to consolidate these contrasting reported uptake coefficients within a single framework for the first time, and explain differences between model predictions and field observations of reactive bromine in the marine environment, as well as making first predictions of HOBr reactive uptake coefficients in volcanic plumes.

3 Results

3.1 The second-order rate constant for aqueous-phase reaction of HOBr with halide ions

In the general acid-assisted mechanism – whereby the rate of reaction of $HOBr_{(aq)}$ (needed in Eq. 2) follows a second-order kinetics – an equilibrium is established between $HOBrX^-_{(aq)}$ and HOBr according to the rate constants of Reactions (R10) and (R11), k_1 and k_{-1} (Eigen and Kustin, 1962). The formation of products, Reaction (R12), involves a transition state $[H_2OBrX_{(aq)}]^{TS}$ that is stabilised by proton donation to the oxygen, with overall rate constant k_H. Moreover, formation of products can also occur at low acid concentrations via a slower pathway, Reaction (R13), followed by fast Reaction (R14), with overall rate constant k_0:

$$HOBr_{(aq)} + X^-_{(aq)} \xrightarrow{k_1} HOBrX^-_{(aq)} \quad \text{(R10)}$$

$$HOBrX^-_{(aq)} \xrightarrow{k_{-1}} HOBr_{(aq)} + X^-_{(aq)} \quad \text{(R11)}$$

$$HOBrX^-_{(aq)} + H^+_{(aq)} \xrightarrow{k_H,[H_2OBrX_{(aq)}]^{TS}} H_2O_{(aq)} + BrX_{(aq)} \quad \text{(R12)}$$

$$HOBrX^-_{(aq)} \xrightarrow{k_0} OH^-_{(aq)} + BrX_{(aq)} \quad \text{(R13)}$$

$$OH^-_{(aq)} + H^+_{(aq)} \xrightarrow{fast} H_2O_{(aq)}. \quad \text{(R14)}$$

According to Reactions (R10–R14), the rate of reaction of $HOBr_{(aq)}$ can be quantified in terms of a second-order rate constant (following Eqs. 3 and 5) where k^{II} is a function of pH, as described by Eq. (6), whose derivation is provided in the Supplement:

$$k^{II} = \frac{k_1 \cdot \left(k_0 + k_H \cdot [H^+_{(aq)}]\right)}{k_{-1} + k_0 + k_H \cdot [H^+_{(aq)}]}. \quad (6)$$

In the limits of high and low acidity (Eqs. 7 and 8), k^{II} is independent of aerosol acidity. For a mid-range acidity ($k_H \cdot [H^+_{(aq)}] \ll k_{-1} + k_0$), k^{II} becomes linearly dependent on

Table 1. Summary of experimental data reported on HOBr uptake coefficient and $HOBr_{(aq)}$ reaction kinetics under tropospheric conditions.

Aerosol or solution	Temperature K	k_{ter} M^{-2} s^{-1}	k^I s^{-1}	k^{II} M^{-1} s^{-1}	γ_{HOBr}	α_{HOBr}	Ref.
$HOBr+Cl^-_{(aq)}$							
HCl-acidified NaCl aerosol with HCl : NaCl = 0.1 : 1	298	–	–	–	> 0.2	–	a
H_2SO_4-acidified sea-salt aerosol with H_2SO_4 : NaCl = 1.45 : 1	296	–	10^3	–	10^{-3}–10^{-2}	–	b
$BrCl_{(aq)}$ solution, pH = 6.4	298	2.3×10^{10}	–	–	–	–	c
$HOBr+Br^-_{(aq)}$							
HOBr uptake onto supersaturated $NaBr_{(aq)}$, $Br^-_{(aq)} > 0.2$ M, at very low $[HOBr_{(g)}]$	296 ± 2	–	–	–	–	0.6	d
$Br_{2(aq)}$ solution, pH = 2.7–3.8	298	1.6×10^{10}	–	–	–	–	e
$Br_{2(aq)}$ solution, pH = 1.9–2.4	298	$1.6(\pm0.2)\times10^{10}$	–	–	–	–	f

[a] Abbatt and Waschewsky (1998); [b] Pratte and Rossi (2006); [c]; Liu and Margarem (2001); [d] Wachsmuth et al. (2002); [e] Eigen and Kustin (1962); [f] Beckwith et al. (1996).

$[H^+_{(aq)}]$ i.e. is acid dependent (Eq. 9). In this mid-acidity regime (only), the acid dependence is equal to the three-body or termolecular rate constant, $k_1 \cdot k_H/(k_{-1}+k_0) = k_{ter}$:

$$k^{II} = k_1 \quad (7)$$

while at high acidity (the limit as $H^+_{(aq)}$ tends to infinity)

$$k^{II} = \frac{k_1 \cdot k_0}{k_{-1}+k_0} \quad (8)$$

and at very low acidity (the limit as $H^+_{(aq)}$ tends to zero)

$$k^{II} = \frac{k_1 \cdot k_0}{k_{-1}+k_0} + \frac{k_1 \cdot k_H \cdot [H^+_{(aq)}]}{k_{-1}+k_0}. \quad (9)$$

Equations (6)–(9) describe k^{II} in terms of four underlying rate constants (k_1, k_{-1}, k_0, k_H) and the aerosol acidity. However, quantifying these underlying rate constants using published data is somewhat challenging given the limited experimental data. This is now attempted below.

3.2 Estimating the underlying rate constants (k_1, k_{-1}, k_0, k_H) for $HOBr+Br^-$ and $HOBr+Cl^-$

A number of aqueous-phase rate constants for the reaction of $HOBr+X^-+H^+$ have been reported: for $HOBr+Br^-_{(aq)}$, Eigen and Kustin (1962) and Beckwith et al. (1996) report termolecular rate constants of $k_{ter} = 1.6\times10^{10}\,M^{-2}\,s^{-2}$ over a pH range of 2.7–3.6 and 1.9–2.4 at 298 K, respectively. These experiments quantified the rate of reaction in the termolecular regime only, although Eigen and Kustin (1962) used a consideration of relative stability constants (e.g. for equilibrium molarity of ternary compounds X_3^- or X_2OH^- relative to X^-, X_2 or XOH) across the halogen series: HOCl+Cl, HOBr+Br and HOI+I to attempt to estimate underlying rate constants.

Using the reported experimental data, k^{II} parameterisations (in terms of the underlying rate constants (k_1, k_{-1}, k_0 and k_H) and acidity according to Eq. (6) derived above) are estimated as follows.

3.2.1 $HOBr+Br^-$

For $HOBr+Br^-$, Eigen and Kustin (1962), proposed order of magnitude estimates of $k_1 = 5\times10^9\,M^{-1}\,s^{-1}$, $k_{-1} = 5\times10^9\,s^{-1}$, $k_H = 2\times10^{10}\,M^{-1}\,s^{-1}$ and $k_0 = 10^4\,s^{-1}$. However, in Fig. 4 of Beckwith et al. (1996), there are indications of acid saturation in their k^{II} rate constant data for $HOBr+Br^-$, seen as curvature in the plots of observed k^{II} vs. acidity. This is also seen in their Fig. 5 where $k^{II}_{observed} \geq 2.3\times10^8\,M^{-1}\,s^{-1}$. We therefore suggest that acid saturation of the reaction between HOBr and Br^- may limit k^{II} to $\sim 5\times10^8\,M^{-1}\,s^{-1}$. We also adjust k_{-1} to $k_{-1} \sim 5\times10^8\,s^{-1}$ on the basis of the reported stability constant $k_1/k_{-1} \sim 1\,M^{-1}$ (Eigen and Kustin, 1962). Since any evidence for acid saturation lies within the reported error bars for the data points this adjustment does not affect our general conclusions about $\gamma_{HOBr+Br}$ in this study.

3.2.2 $HOBr+Cl^-$

For $HOBr+Cl^-_{(aq)}$, Liu and Margarem (2001) report a three-body rate constant of $2.3\times10^{10}\,M^{-2}\,s^{-2}$ in buffered aerosol at pH = 6.4 and 298 K. Pratte and Rossi (2006) also derived estimates for first-order rate constants for reaction of $HOBr_{(aq)}$ from their uptake coefficient experiments. We re-evaluate these data below to improve quantification of the reaction kinetics of $HOBr+Cl^-$.

For $HOBr+Cl^-$, the underlying rate constants (k_1, k_{-1}, k_H, k_0) are estimated as follows. The rate constant k_1 is derived from the estimation of k^{II} at acid saturation (Eq. 7). For this, we estimated k^{II} at pH −1 to 0 from experiments of Pratte and Rossi (2006), Table 2. These new estimates of

k^{II} are derived from first-order k^{I} rate constants for the reaction of $HOBr_{(aq)}$, reported by Pratte and Rossi (2006), where $[Cl^{-}_{(aq)}]$ is calculated by the E-AIM model from experimental conditions – E-AIM predicts that chloride concentrations are reduced under the experimental conditions as a consequence of the acid displacement of $HCl_{(g)}$ (see further discussion in the Supplement). We find that $k^{II} \sim 10^4\,M^{-1}\,s^{-1}$ over pH −1 to 0, see Table 2 for details. We note that in their reporting of k^{I} rate constants from their uptake experiments, Pratte and Rossi (2006) assumed an accommodation coefficient of either $\alpha_{HOBr} = 0.2$ or $\alpha_{HOBr} = 0.02$. Given that experiments on $NaBr_{(aq)}$ aerosol have identified an accommodation coefficient for HOBr on $NaBr_{(aq)}$ particles of 0.6 (Wachsmuth et al., 2002), the k^{II} data derived assuming $\alpha_{HOBr} = 0.2$ are likely more representative. Nevertheless, either case yields an estimate for $k^{II} \sim 10^4\,M\,s^{-1}$ over pH = 0 to −1. A second estimate for k^{II} is made from the reported three-body rate constant of $2.3 \times 10^{10}\,M^{-2}\,s^{-2}$ at pH = 6.4, by setting $k^{II} = k_{ter} \cdot [H^{+}_{(aq)}]$. This yields $k^{II} = 9 \times 10^3\,M^{-1}\,s^{-1}$ at pH 6.4.

Thus, collectively these two data sets at pH = 6.4 and 0 to −1 suggest that k^{II} is acid saturated at $\sim 10^4\,M\,s^{-1}$ at pH ≤ 6. Based on this value for k^{II} at acid saturation (where $k^{II} = k_1$) we set $k_1 = 1.2 \times 10^4\,M\,s^{-1}$ as an average estimate, which is less than k_1 for HOBr+Br^-, and which is consistent with the greater nucleophile strength of Br^- compared to Cl^-. We fix $k_H = 2 \times 10^{10}\,M^{-1}\,s^{-1}$, equal to that estimated by Eigen and Kustin (1962)) for HOBr+Br^-, noting that this reaction is likely close to the diffusion limit. Our value of k^{II} for HOBr+Cl^- at low acidity ($=(k_1.k_0)/(k_0 + k_{-1})$) is a similar order of magnitude to the k^{II} estimate for HOCl+Cl^- ($\leq 0.16\,M^{-1}\,s^{-1}$, see Gerritsen and Margarem, 1989) or perhaps slightly higher (because the less electronegative Br of HOBr may be more susceptible to nucleophilic attach than HOCl), but is substantially less than the k^{II} estimate for HOBr+Br^- ($10^4\,M^{-1}\,s^{-1}$, Eigen and Kustin, 1962) at low acidity, and consistent with Cl^- being a weaker nucleophile than Br^-. Overall, as a value for the low acidity k^{II} rate constant, $(k_0 \cdot k_1)/(k_1 + k_{-1}) = 10^1\,M^{-1}\,s^{-1}$ seems reasonable.

A similar analysis based on the three-body rate constant of $2.3 \times 10^{10}\,M^{-2}\,s^{-1}$ (Liu and Magarem, 2001). yields $k_0 = 2 \times 10^1\,s^{-1}$ and $k_{-1} = 1.1 \times 10^4\,s^{-1}$. These estimates for the underlying rate constants for HOBr+Cl^- are rather uncertain; nevertheless the most important result is the occurrence of acid saturation of k^{II} for HOBr+Cl^-, which the experimental data limits to $\sim 10^4\,M\,s^{-1}$ at pH ≤ 6.

3.3 A new parameterisation for the k^{II} for HOBr+Br^- and HOBr+Cl^-

The underlying rate constants (k_1, k_{-1}, k_H, k_0) for reaction of HOBr+Br^- and HOBr+Cl^- estimated above are summarised in Table 3. Our parameterisation for k^{II} based on these data, with k^{II} defined by Eq. (6) is shown in Fig. 1 as a function of aerosol acidity, alongside the experimental

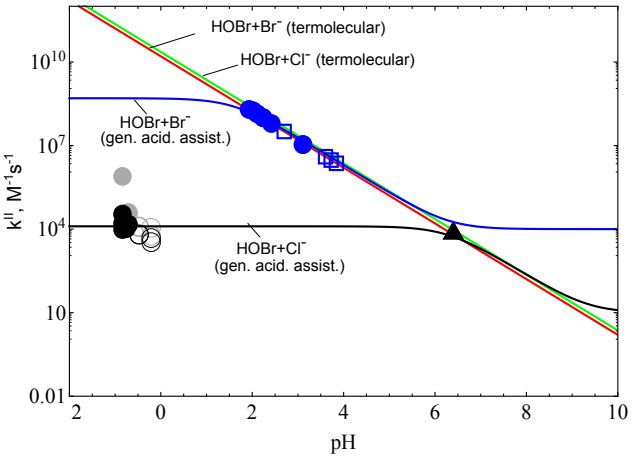

Figure 1. Second-order rate constants for the reaction of HOBr with Br^- and Cl^- as a function of pH. Experimental estimates for k^{II} for HOBr+Br^- derived from data from Eigen and Kustin (1962) and Beckwith et al. (1996) (blue squares and circles respectively) are shown alongside model estimate (blue line) according to the acid-assisted mechanism. The red line denotes the k^{II} rate constant assuming termolecular kinetics across all pH. Experimental estimates for k^{II} for HOBr+Cl^- derived from data from Liu and Margarem (2001) at pH = 6.4 (black triangle) and Pratte and Rossi (2006) at pH −1 to 0 (black and grey discs for data at RH = 77–80 %, open circles for RH = 85–90 %), are shown alongside model estimate (black line) according to the general acid-assisted mechanism. The green line denotes the k^{II} rate constant assuming termolecular kinetics across all pH.

values for k^{II} derived from the reported experimental data from Eigen and Kustin (1962), Beckwith et al. (1996), Liu and Margarem (2001) and Pratte and Rossi (2006) (see Table 2). As expected, the k^{II} parameterisations for HOBr+Br^- and HOBr+Cl^- exhibit three distinct regimes: k^{II} is independent of acidity at high pH. k^{II} is dependent on acidity for a medium pH range, where the rate constant $k^{II} = k_{ter} \cdot [H^{+}_{(aq)}]$, and in this regime the rate constant is termolecular. At high acidity, k^{II} becomes acid independent ($k^{II} = k_1$), yielding an acid-saturated k^{II} that is lower for HOBr+Cl^- than HOBr+Br^- given the weaker nucleophile strength.

Also shown in Fig. 1 is the termolecular approach to HOBr kinetics assumed to date, which predicts acid-dependent k^{II} over all parameter space. Clearly, the termolecular assumption for HOBr kinetics is only valid in the termolecular regime, between pH 1–6 for HOBr+Br^-, and > pH 6 for HOBr+Cl^-. At high acidity, the termolecular approach overestimates the rate constant compared to the k^{II} parameterisation by several orders of magnitude. The disagreement is greatest for HOBr+Cl^-, where the termolecular approach overestimates the k^{II} rate constant by a factor of 10^3 at pH = 3 and 10^6 at pH = 0). Of interest is the effect of our revised parameterisation on the HOBr reactive uptake coefficient. Below we compare the reactive uptake coefficients

Table 2. Extraction of second-order rate constant values, k^{II} from reported experimental data. For HOBr+Br, k^{II} is derived from reported termolecular rate constants using $k^{II} = k_{ter} \cdot [H^+_{(aq)}]$. For HOBr+Cl−$k^{II}$ is derived from a reported termolecular rate constant using $k^{II} = k_{ter} \cdot [H^+_{(aq)}]$ and from reported first-order rate constant data, k^I using $k^{II} = k^I / [Cl^-_{(aq)}]$. Molarity and activity of $Cl^-_{(aq)}$ and $H^+_{(aq)}$ were calculated using the E-AIM model at 298.15 K. See Sect. 2.

Experiment	T K	RH %	wt% H_2SO_4	pH	$Cl^-_{(aq)}$ activity	k_{ter} M	k^I s^{-1} M^{-2} s^{-1}		k^{II} M^{-1} s^{-1}		Ref.
HOBr+Br$^-$											
$Br_{2(aq)}$	293	–	–	2.7–3.6	–	1.6×10^{10}	–		$4. \times 10^6$–3.2×10^7		a
$Br_{2(aq)}$	298	–	–	1.9–2.4	–	$1.6(\pm 0.2) \times 10^{10}$	–		6.1×10^7–1.9×10^8		b
HOBr+Cl$^-$											
$BrCl_{(aq)}$	298	–	–	6.4	2.0	2.3×10^{10}	–		8.8×10^3		c
							($\alpha = 0.2$*)	($\alpha = 0.02$*)	($\alpha = 0.2$*)	($\alpha = 0.02$*)	
H_2SO_4 : NaCl	296	77	31.7	−0.84	0.056		922	1855	1.6×10^4	3.3×10^4	d
(1.45 : 1)	296	79	30.00	−0.75	0.069		1050	2510	1.5×10^4	3.6×10^4	
	296	80	29.1	−0.71	0.076		1140	3010	1.5×10^4	3.9×10^4	
	296	85	24.2	−0.48	0.127		800	1485	6.3×10^3	1.2×10^4	
	296	90	17.7	−0.21	0.209		995	2355	4.8×10^3	1.1×10^4	
H_2SO_4 : NaCl (1.45 : 1)NSS	296	77	31.7	−0.84	0.056		1960	44000	3.5×10^4	7.8×10^5	d
H_2SO_4 : NaCl	296	77	31.7	−0.84	0.056		545	795	9.6×10^3	1.4×10^4	d
(1.45 : 1) RSS	296	79	30.00	−0.75	0.069		720	1225	1.0×10^4	1.8×10^4	
	296	80	29.1	−0.71	0.076		1090	2600	1.4×10^4	3.4×10^4	
	296	85	24.2	−0.48	0.127		815	1580	6.4×10^3	1.2×10^4	
	296	90	17.7	−0.21	0.209		710	1210	3.4×10^3	5.8×10^3	

[a] Termolecular rate constant reported by Eigen and Kustin (1962). [b] Termolecular rate constant reported by Beckwith et al. (1996). [c] Termolecular rate constant reported by Liu and Magarem (2001) for buffered aerosol containing $Cl^-_{(aq)}$ at pH = 6.4 at $T = 298$ K. [d] First-order rate constant, k^I_{rxn} data reported by Pratte and Rossi (2005) for aerosol mixture at H_2SO_4 : NaCl = 1.45, for laboratory sea salt, natural sea salt (nss) or recrystallised sea salt (rss). Pratte and Rossi (2006) assumed two different accommodation coefficients ($\alpha = 0.2$, $\alpha = 0.02$) in the derivation of k^I_{rxn} values from their uptake experiments, the former being closest to $\alpha = 0.6$ reported on $NaBr_{(aq)}$ aerosol by Wachsmuth et al. (2002).

Table 3. Underlying rate constant data (k_1, k_{-1}, k_0, k_H) used in k^{II} parameterisations of Fig. 1.

	HOBr+Br	HOBr+Cl
k_1, M^{-1} s^{-1}	5×10^8 [b,a]	1.2×10^4 [c]
k_{-1}, s^{-1}	5×10^8 [b,a]	1.1×10^4 [c]
k_0, s^{-1}	10^4 [a]	2×10^1 [c]
k_H, M^{-1} s^{-1}	2×10^{10} [a]	2×10^{10} [c]

[a] Estimated in this study, [b] derived from Eigen and Kustin (1962), [c] derived from Kumar and Margerum (1987).

of HOBr calculated with our revised k^{II} parameterisation to experimental uptake coefficients reported under laboratory conditions. In Sect. 5 we present calculations of the HOBr reactive uptake coefficient for marine and volcanic plume conditions and discuss the implications for reactive halogen chemistry in these environments.

3.4 Comparison of our model with experimental uptake coefficient data

As discussed in the Introduction, discrepancies exist in the reported reactive uptake coefficients for HOBr on acidified sea-salt aerosol. Abbatt and Waschewsky (1998) observed a strong pH dependence of the uptake onto sodium chloride aerosol, being 1.5×10^{-3} for neutral, unbuffered sodium chloride aerosol, rising to > 0.2 for aerosols acidified to pH 0.3 by the addition of HCl, i.e. close to the accommodation coefficient ($\alpha = 0.6 \pm 0.2$, Wachsmuth et al., 2002). The role of H^+ species in the reactive uptake process was further demonstrated by the high uptake coefficient of > 0.2 on aerosols buffered to pH 7 by a NaH_2PO_4/Na_2HPO_4 buffer. In contrast, Pratte and Rossi (2006) measured reactive uptake coefficients on H_2SO_4-acidified sea-salt aerosol to be $\sim 10^{-2}$ at H_2SO_4 : NaCl = 1.45 : 1, with an RH dependence (finding $\gamma_{HOBr} \sim 10^{-3}$ at RH < 70 %).

We have calculated the reactive uptake coefficients for HOBr for the conditions of these two laboratory experiments using our new parameterisation for k^{II} and the E-AIM model to determine aerosol composition.

Below we show that the origin for this wide discrepancy between measured HOBr uptake onto acidified bromide aerosol and chloride aerosol lies partly in the difference in reactivity of HOBr towards Br^- and Cl^-, but also in differences in aerosol composition in the two studies: HCl-acidified sea-salt aerosol retains high $Cl^-_{(aq)}$ concentrations, whereas H_2SO_4-acidified sea-salt aerosol undergoes HCl displacement, lowering $Cl^-_{(aq)}$ concentrations. This acid displacement of HCl leads to a lowering of the reactive uptake coefficient for HOBr on H_2SO_4-acidified aerosol.

3.4.1 High uptake coefficient on HCl-acidified sea-salt aerosol

On HCl-acidified $NaCl_{(aq)}$ aerosol, Abbatt and Wachewsky (1998) measured the uptake coefficient of

HOBr to be > 0.2. We calculate the uptake coefficient for HOBr+Cl^- under these experimental conditions for which a chloride concentration of 6.6 M is predicted according to E-AIM (see details in Sect. S3.1.1 of Supplement and Table 4). For particles of 1 µm radius at 298 K, both our new parameterisation for k^{II} and the termolecular approach to HOBr+Cl^- kinetics yield a high uptake coefficient, $\gamma_{HOBr+Cl} \sim 0.6$, and thus are consistent with the experimental findings, see Table 4.

3.4.2 Low uptake coefficient on H_2SO_4-acidified sea-salt aerosol with RH dependence

On H_2SO_4-acidified sea-salt aerosol, Pratte and Rossi (2006) measured the uptake coefficient of HOBr to be $\sim 10^{-2}$ at $H_2SO_4 : NaCl = 1.45 : 1$, with an RH dependence (finding $\gamma_{HOBr} \sim 10^{-3}$ at RH < 70 %). Using our parameterisation, we calculate the uptake coefficient for HOBr+Cl^- under these experimental conditions, at 298 K, and with variable RH (see details in Sect. S3.1.2 of the Supplement and Table 4). We assume a solubility of HOBr in sulfuric acid of 363 M atm^{-1} at 296 K (following Pratte and Rossi, 2006 based on Iraci et al., 2005), and calculate a HOBr diffusion coefficient in sulfuric acid of 5.5×10^{-6} cm^2 s^{-1} and 1.0×10^{-5} cm^2 s^{-1} at 50 and 80 % RH (48 and 29 wt%H_2SO_4) respectively. E-AIM predicts the aerosol $Cl^-_{(aq)}$ concentrations to be 0.004 M L^{-1} and 0.08 M L^{-1} at 50 and 80 % RH respectively, see Table 4.

The new parameterisation for k^{II} yields uptake coefficients for HOBr+Cl^- of 4.4×10^{-3} at 50 % RH and 7.6×10^{-2} at 80 % RH, in broad agreement to the low uptake coefficients reported by Pratte and Rossi (2006); 1.0 ± 10^{-2} at RH ≥ 76 %. Such agreement is to some extent not surprising, given the usage of k^I reported at RH = 77–90 % from the same Pratte and Rossi (2006) experiments to derive an estimate for k^{II} at acid saturation (see Sect. 3 and Fig. 1). Nevertheless, the uptake calculations confirm and provide a first explanation for the RH dependence of the uptake coefficient as reported by Pratte and Rossi (2006). The model indicates that the underlying cause of this trend is greater $[Cl^-_{(aq)}]$ at higher RH, given higher solubility of HCl at the lower wt%H_2SO_4 at high RH. This is further shown by Fig. 2 which compares the modelled and observed RH dependence of the uptake coefficient of HOBr across all reported data from 40 to 90 % RH, demonstrating broad agreement in the trend (noting that discrepancies may result from impurities within the sea-salt solution or uncertainties within the parameterisations used in the uptake model). These findings are in contrast to the termolecular approach to k^I that yields an uptake coefficient of 0.6 at both RH values – substantially overestimating γ_{HOBr} by at least a factor of 20 (see Table 4). This is because the termolecular approach assumes acid-dependent k^{II} across all pH, leading to an extremely high rate constant for the reaction of HOBr+Cl^- at pH −1 to 0, and a very fast rate of reaction of HOBr with Cl^-. Even though Cl^- concentrations are depleted by acid displacement, the assumed increased rate constant at low pH overcompensates for this effect.

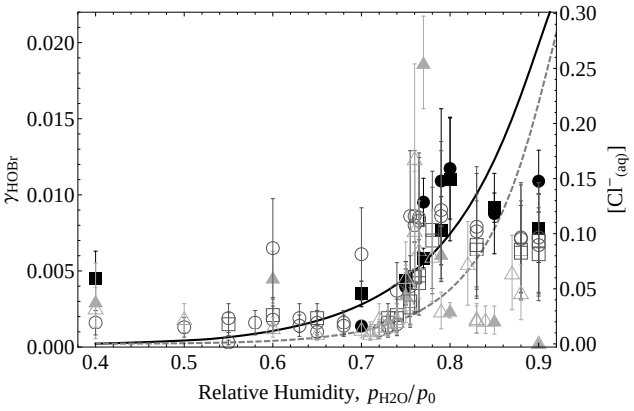

Figure 2. Dependence of reactive uptake coefficient for HOBr on relative humidity (RH) in the experiments of Pratte and Rossi (2006) on H_2SO_4-acidified sea-salt aerosol ($H_2SO_4 : NaCl = 1.45 : 1$) at 296 K, on acidified sea salt (circles), recrystallised sea salt (squares) and natural sea salt (triangles), under two experimental setups: (i) the observed rate of $HOBr_{(g)}$ decay for a measured aerosol size distribution, with effective radius ranging over 165–183 nm (filled shapes), and (ii) a survey type mode with HOBr depletion monitored as a function of RH (unfilled shapes, with reported error estimated at 30–50 %) over a constant reaction time. Also shown is the modelled uptake coefficient for HOBr (black line), and the $Cl^-_{(aq)}$ molarity (dotted line) as used within the uptake calculation.

In conclusion, our new k^{II} parameterisation for the kinetics of HOBr+X− yields uptake coefficients in agreement with reported laboratory data, and – for the first time – reconciles differences between reported uptake on HCl-acidified and H_2SO_4-acidified sea-salt aerosols, within a single framework.

4 Implications for BrO chemistry in the marine and volcanic environments

4.1 Declining uptake coefficients on progressively H_2SO_4-acidified sea-salt aerosol

Using the revised HOBr reaction kinetics (Fig. 1), the HOBr+Br^- and HOBr+Cl^- reactive uptake coefficients are now re-evaluated for a model sea-salt aerosol that undergoes progressive H_2SO_4 acidification (Fig. 3) and compared to calculations using the termolecular approach. We investigate how the reductions in halide ion concentrations caused by the $H_2SO_{4(aq)}$ addition (through both acid-displacement reactions that deplete $[Cl^-_{(aq)}]$, and dilution of $[Br^-_{(aq)}]$ by $H_2SO_{4(aq)}$ volume) impact γ_{HOBr} at low pH.

A particle radius of 1 or 0.1 µm is assumed in the uptake calculation. Temperature is set to 298 K and RH = 80 % (above deliquescence). For aerosol that is alkaline or

Table 4. Predicted uptake coefficients compared to reported uptake on experimental aerosol. * Br^- concentration prior to aerosol dehumidifying – reported reduction in volume during dehumidifying indicates actual concentration may be a factor of ∼ 3 higher; ** reported modal radius, although particles >0.2 µm exist within the size spectrum.

Experimental aerosol:	NaBr aerosol Wachsmuth et al. (2002) supersaturated $NaBr_{(aq)}$	HCl-acidified NaCl aerosol Abbatt and Waschewsky (1998) HCl / NaCl = 0.1 : 1	H_2SO_4-acidified sea-salt aerosol Pratte and Rossi (2006) H_2SO_4 / NaCl = 1.45 : 1	
γ_{HOBr}: observed	0.6 ± 0.2	> 0.2	$(0.1–0.3) \times 10^{-2}$ at RH 40 to 70 %	$(1.0 \pm 0.2) \times 10^{-2}$ at RH ≥ 76 %
Uptake model parameters:				
Temperature	298.15	298.15	298.15	298.15
α (accommodation coefficient)	0.6	0.6	0.6	0.6
Na concentration (µmol m^{-3})	–	0.2	0.8	0.8
RH, %	80	76	50	80
$[Br^-_{(aq)}]$, M	> 0.2*	–	–	–
$[Cl^-_{(aq)}]$, M (E-AIM)	–	6.6	4.4×10^{-3}	7.6×10^{-2}
$[H^+_{(aq)}]$, M (E-AIM)	$\sim 2 \times 10^{-6}$	2.3	83	5
pH	∼ 6	−0.3	−1.9	−0.7
k^{II}, $M^{-1}\,s^{-1}$	3×10^4	10^4	10^4	10^4
k_{ter}, $M^{-2}\,s^{-1}$	1.6×10^{10}	2.3×10^{10}	2.3×10^{10}	2.3×10^{10}
Particle radius, µm	> 0.03**	1.	∼ 0.17	∼ 0.17
wt%H_2SO_4	–	–	48	29
HOBr solubility, M atm^{-1}	6.1×10^3	6.1×10^3	364	364
HOBr diffusion constant, $cm^2\,s^{-1}$	1.42×10^{-5}	1.42×10^{-5}	5.5×10^{-6}	1.0×10^{-5}
γ_{HOBr}: old approach (where $k^I = k_{ter} \cdot [X^-_{(aq)}] \cdot [H^+_{(aq)}]$)	$0.1 < \gamma_{HOBr} \leq 0.6$	0.6	0.6	0.6
γ_{HOBr}: new approach (where $k^I = k^{II} \cdot [X^-_{(aq)}]$)	$0.1 < \gamma_{HOBr} \leq 0.6$	0.6	2×10^{-4}	7×10^{-3}

only weakly acidic (pH 12 to pH 4), uptake coefficients were calculated assuming a fixed sea-salt composition with $[Cl^-_{(aq)}] = 5.3\,Mol\,L^{-1}$ and $[Br^-_{(aq)}] = 0.008\,Mol\,L^{-1}$, with pH varied between 4 and 12 (E-AIM was not used, given the very low degree of H_2SO_4 acidification). For more strongly acidified sea salt, across H_2SO_4 : Na ratios from 0.05 to 400 (pH 4 to −0.87 for the model aerosol conditions), E-AIM was used to determine the extent of acid displacement of HCl from acidified $NaCl_{(aq)}$ aerosol, with aerosol $Br^-_{(aq)}$ determined using an effective Henry's law solubility for HBr (see predicted composition in Supplement Sect. S3.2).

Figure 4 shows that the calculated reactive uptake for $HOBr+Br^-$ and $HOBr+Cl^-$ increases with increasing acidity over pH 4–12 for the uptake coefficient for 0.1 and 1 µm radius particles, similar to that previously reported using the termolecular approach. The alkaline to acid transition in γ_{HOBr} reflects the increase in the underlying $HOBr_{(aq)}$ k^I rate constant with acidity due to the onset of the acid-assisted mechanism, Fig. 1, as well as the decrease of HOBr partitioning to BrO^-. The $\gamma_{HOBr+Cl}$ reaches values close to the accommodation limit by pH ≤ 8 (for 1 µm radius particles) or pH ≤ 7 (for 0.1 µm radius particles) while $\gamma_{HOBr+Br}$ reaches values close to the accommodation limit by pH ≤ 5 (for 1 µm radius particles) or pH ≤ 4 (for 0.1 µm radius particles).

In the high-acidity regime, the acid saturation of k^{II} can cause γ_{HOBr} to plateau at a level slightly lower than α_{HOBr} (e.g. in $\gamma_{HOBr+Cl}$ at pH ∼ 4), in contrast to the termolecular approach. Overall, for slightly acidified sea-salt aerosol, reactive uptake of HOBr is driven primarily by $\gamma_{HOBr+Cl}$. The $\gamma_{HOBr+Br}$ reaches similar values to $\gamma_{HOBr+Cl}$ at pH ∼ 3–4 for the specific model aerosol conditions of this study.

However, as the degree of acidification by H_2SO_4 increases, the uptake coefficient for $HOBr+Cl^-$ begins to decline at pH < 4. This is due to acid-displacement reactions that convert $Cl^-_{(aq)}$ into $HCl_{(g)}$, thereby lowering $[Cl^-_{(aq)}]$. This leads to $\gamma_{HOBr+Cl-} < \gamma_{HOBr+Br-}$, i.e. HOBr reactive uptake becomes driven by $HOBr+Br^-$ below a pH of ∼ 2 for the specific aerosol conditions of this study. As H_2SO_4 : Na ratio increases further and pH decreases further, the uptake coefficient for $HOBr+Br^-_{(aq)}$ also begins to decline. This is principally due to the dilution of $Br^-_{(aq)}$ by the additional volume of $H_2SO_{4(aq)}$ that becomes important particularly at very high H_2SO_4 : Na (see E-AIM calculations in the Supplement).

Notably, the declines in uptake coefficients are greatest for smaller particles, for which there is a greater probability that $HOBr_{(aq)}$ may diffuse across the particle and be released to the gas phase, without any aqueous-phase reaction occurring.

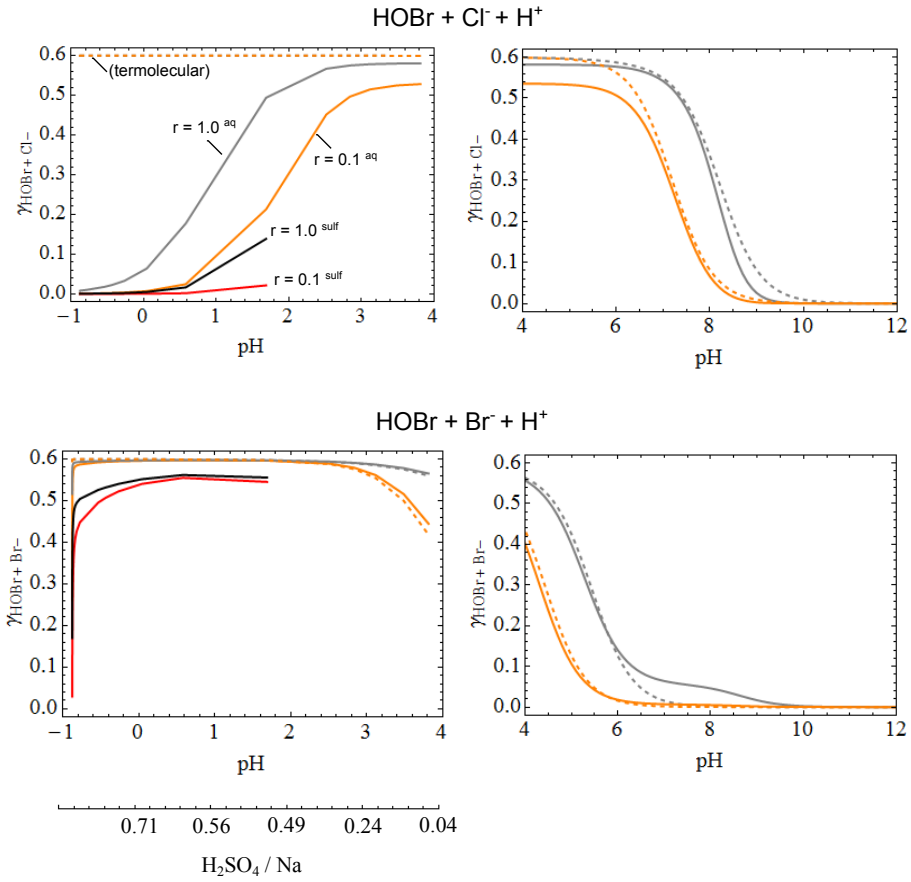

Figure 3. Variation in the HOBr uptake coefficient with pH, for reaction of HOBr with (upper) Cl^- and (lower) Br^- on H_2SO_4-acidified sea-salt aerosol. Grey and orange lines denote uptake onto 1 and 0.1 µm radius particles, respectively. Black and red lines denote uptake onto 1 and 0.1 µm radius particles calculated using H* and D_l parameterisations for sulfuric acid (rather than water), shown only for H_2SO_4 : Na ratios greater than 0.5. Relative humidity is set to 80 % and Na concentration 1.3×10^{-7} moles m^{-3} (equivalent to a PM_{10} of 10 µg m^{-3} in the marine environment, Seinfeld and Pandis, 1998). For comparison, uptake coefficients calculated assuming termolecular kinetics are also shown (dashed lines).

The uptake coefficients are also further reduced if parameterisations for the solubility of HOBr in $H_2SO_{4(aq)}$ is assumed in the uptake equation rather than that for water. The exact point of transition between these two parameterisations is not well constrained, but it is clear that the $H_2SO_{4(aq)}$ parameterisations become more applicable than water with greater acidification, and must certainly be more relevant at high H_2SO_4 : Na. The lower solubility of HOBr in $H_2SO_{4(aq)}$ acts to decrease the uptake coefficient, and is found to have a stronger impact on γ_{HOBr} than the slower rate of diffusion of $HOBr_{(aq)}$ in H_2SO_4.

In summary, following a rise over the alkaline–acid transition, our revised HOBr kinetics yields HOBr reactive uptake coefficients that subsequently decline on progressively H_2SO_4-acidified sea-salt aerosol. For the aerosol concentration assumed, the uptake coefficient on the 0.1 µm radius particles declines to $\gamma_{HOBr+Br} < 0.03$ at a H_2SO_4 : Na ratio of 400 : 1, indicating that the reactive uptake of HOBr on highly acidified sub-micrometre particles is extremely low, Fig. 3. These decreases in uptake coefficient with increasing aerosol acidity are not captured by calculations that assume termolecular kinetics. As stated in the previous section, this is because the termolecular approach assumes that the HOBr rate constant is acid dependent across all pH, and does not consider acid saturation of the rate constant.

4.2 Implications for BrO chemistry in the marine boundary layer

Figure 4 shows clearly that higher acidity does not necessarily lead to faster production of reactive bromine. It is well known that acidity is required for reactive bromine formation to occur: $H^+_{(aq)}$ is consumed in the reaction, therefore a source of acidity is required to sustain prolonged BrO formation chemistry. Further, under alkaline conditions HOBr dissociates into less reactive OBr^-. However, the γ_{HOBr} dependency on acidity shown here suggests that additional aerosol acidification by $H_2SO_{4(aq)}$ can act as a limitation to the formation

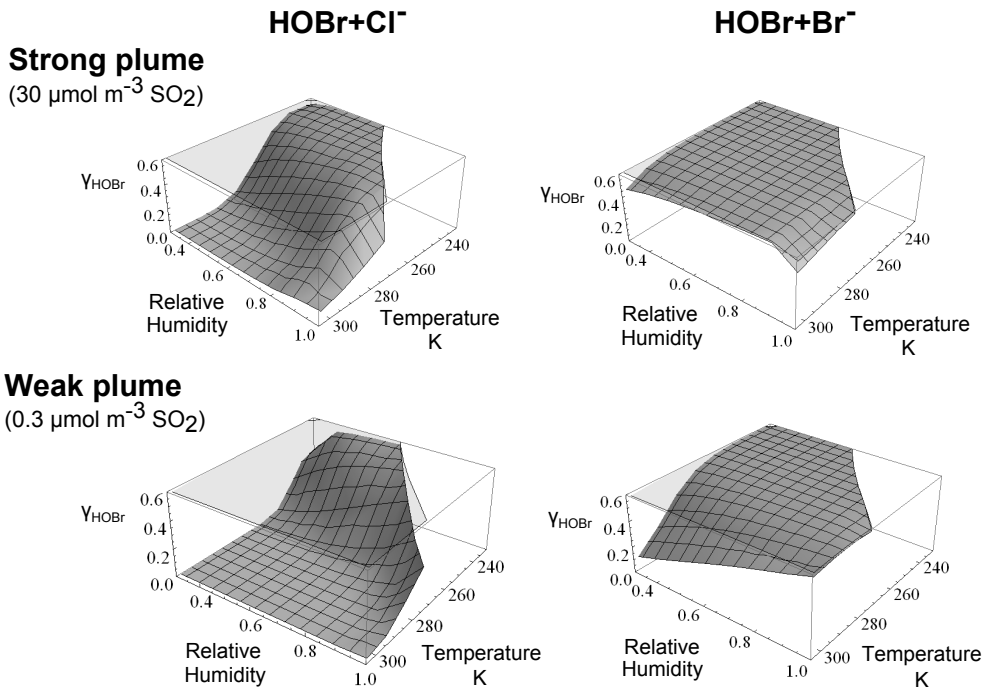

Figure 4. HOBr+Cl^- and HOBr+Br^- reactive uptake coefficients onto volcanic sulfate aerosol particles of 1 µm radius, calculated using our revised HOBr kinetics. Calculations are performed for a typical Arc or subduction zone volcanic plume composition containing a $(SO_2) : HCl : H_2SO_4 : HBr$ molar ratio mixture of $1 : 0.5 : 0.01 : 0.00075$. The plume strength is 30, or 0.3 µmol m^{-3}, equivalent to approximately 1 or 0.01 ppmv SO_2 at 4 km altitude (US standard atmosphere). Conversely, uptake coefficients calculated using the termolecular approach yield high accommodation-limited values across all parameter space (light grey).

of reactive bromine via HOBr uptake, particularly for small particle sizes.

This leads to the following implications for BrO chemistry in the marine environment, where both supra-micron and sub-micron particles are reported, the former typically being moderately acidified perhaps with some Cl depletion, and the latter being dominated by H_2SO_4 with only a trace quantity of sea salt (e.g. Keene et al., 2002):

Firstly, the reactive uptake of HOBr is driven by reaction with Br^- as $\gamma_{HOBr+Cl}$ is reduced on H_2SO_4-acidified (Cl^--depleted) sea-salt aerosol. This leads to a negative feedback in the uptake coefficient for HOBr with BrO chemistry evolution over time, as the conversion of $Br^-_{(aq)}$ to $Br_{2(g)}$ acts to decrease aerosol $[Br^-_{(aq)}]$, reducing subsequent values of $\gamma_{HOBr+Br}$. This negative feedback for $\gamma_{HOBr+Br}$ will play a much more significant role for overall HOBr reactive uptake according to our revised HOBr kinetics than has been assumed by model studies to date based on the termolecular approach (for which $\gamma_{HOBr+Cl} \geq \gamma_{HOBr+Cl}$).

Secondly, very low reactive uptake coefficients for both HOBr+Br^- and HOBr+Cl^- are predicted for sub-micron particles at high $H_2SO_4 : Na$ ratios (e.g. $\gamma_{HOBr} < 0.03$, see Fig. 4). Such low γ_{HOBr} is proposed as a first explanation for the absence of observable $Br^-_{(aq)}$ depletion in sub-micron $H_2SO_4^-$-dominated particles in the marine environment, in contrast to supra-micron particles where $Br^-_{(aq)}$ depletion is observed and interpreted as evidence of HOBr reactive uptake to form reactive bromine (Sander et al., 2003). Indeed, observations find the submicron H_2SO_4-dominated aerosol to be enriched in $Br^-_{(aq)}$ relative to expected concentrations based on the particle Na^+ content (Sander et al., 2003). A plausible explanation is that the release of $Br_{2(g)}$ from the supra-micron particles leads to the continual formation of gas-phase reactive bromine species of which a proportion will ultimately be deposited back to (both types of) marine aerosols as a source of $Br^-_{(aq).}$ The net effect is for $Br^-_{(aq)}$ concentrations to become enhanced (relative to Na) in the submicron aerosol where γ_{HOBr} is low simultaneous to becoming depleted in the supra-micron aerosol where γ_{HOBr} is high. For the former, an upper limit must exist to the extent Br enrichment can occur whilst maintaining the relatively low $\gamma_{HOBr+Br-}$. Importantly, this argumentation is only possible using our new uptake calculations based on k^I calculated using revised HOBr kinetics in terms of k^{II}, as the termolecular approach predicts high HOBr reactive uptake for both particle types. We encourage our new rate constant calculations for HOBr reactive uptake to be incorporated into numerical models to test and quantify potential submicron aerosol Br^- enrichment via this proposed mechanism.

We further suggest that both of the abovementioned factors may also contribute underlying reasons for the reported over-prediction by numerical models of BrO cycling in the marine environment (Sander et al., 2003; Smoydzin and von Glasow, 2007; Keene et al., 2009). Inclusion of the new HOBr kinetics into such models will allow this hypothesis to be tested and quantified.

4.3 Reactive uptake of HOBr on volcanic aerosol

HOBr reactive uptake coefficients are now calculated for the first time onto aerosol in a halogen-rich volcano plume, using the k^{II} parameterisations for HOBr+Br^- and HOBr+Cl^-. Using the volcanic aerosol composition predicted by E-AIM (based on Etna emission scenario, see Sect. S3.3 of the Supplement), uptake coefficients for HOBr+Br^- and HOBr+Cl^- are calculated across tropospheric temperature and relative humidity, for two plume dilutions (30 and 0.3 µmol m^{-3}, which are equivalent to ∼ 1 ppmv, and 0.01 ppmv SO_2 at 4 km altitude in US standard atmosphere), and assuming a particle radius of 1 µm, Fig. 4. There exists no experimental information regarding the temperature dependence of k^{II} for HOBr+X. Here it is assumed that the variation k^{II} with temperature over 230–300 K is small compared to the temperature dependence of the HOBr and HX solubilities (which vary by several orders of magnitude over the parameter space).

High HOBr uptake coefficients are predicted at low tropospheric temperatures: $\gamma_{HOBr+Br-} \approx \gamma_{HOBr+Cl-} \approx 0.6$. The uptake coefficient decreases markedly with increasing temperature for $\gamma_{HOBr+Cl-}$ and also decreases for $\gamma_{HOBr+Br-}$ in the most dilute plume scenario. The inverse temperature trend in γ_{HOBr} is caused by a lower solubility of HX in sulfuric acid particles at higher tropospheric temperatures (particularly for HCl), augmented by a similar temperature trend in the solubility of $HOBr_{(aq)}$. The variation with plume dilution is explained by the fact that lower gas-to-aerosol partitioning yields lower $[X^-_{(aq)}]$ in the dilute plume scenarios, thus a lower $k^I = k^{II} \cdot [X^-_{(aq)}]$ in the uptake equation, and hence a reduced γ_{HOBr}. Figure 4 also illustrates a weak dependence of the uptake coefficients on relative humidity. This is due to increasing solubility of the halides with RH or lower wt%H_2SO_4 (potential RH dependence of HOBr solubility is not considered in the parameterisations, see the Supplement). As for the marine aerosol study, reductions in γ_{HOBr} are more pronounced for particles of smaller radii (data not shown), as the probability for diffusion across the particle without reaction is higher. According to Fig. 4, $\gamma_{HOBr+Br-}$ is equal to or exceeds $\gamma_{HOBr+Cl-}$ under all temperature and humidity scenarios for the composition of the Etna emission. This is driven by higher k^I in the uptake calculation (where $k^I = k^{II} \cdot [X^-]$ with k^{II} a function of pH), due to the greater saturation value k^{II} for HOBr+Br^- at high acidity, and the higher solubility of HBr compared to HCl. Again it is important to note that this uptake re-evaluation using revised HOBr kinetics differs from that calculated using the termolecular approach (also shown in Fig. 4) which yields high and typically accommodation-limited HOBr uptake coefficients throughout the parameter space. Indeed, this is due to the fact that with the termolecular approach ($k^I = k_{ter} \cdot [H^+_{(aq)}] \cdot [X^-_{(aq)}]$) the increased value of k_{ter} at high acidity more than compensates for the acidity-driven decreases in X, thus yielding high k^I and high γ_{HOBr}.

Figure 4 shows that in concentrated plumes near to the volcanic source, the aqueous-phase halide concentrations are sufficiently high that $\gamma_{HOBr+Br-}$ is accommodation limited. Rapid formation of BrO is expected to occur. This is consistent with observations of volcanic BrO at numerous volcanoes globally (e.g. Bobrowski and Platt, 2007; Boichu et al., 2011, and references therein), including emissions from both low- and high-altitude volcanoes, explosive eruptions and from passive degassing. However, it is anticipated that the reactive uptake coefficient for HOBr+Br^- will be reduced as BrO chemistry progresses causing $Br^-_{(aq)}$ concentrations to decline (due to conversion of HBr into reactive bromine). This will likely slow the BrO cycling in the more evolved plume. Plumes will also become more dilute over time due to dispersion. Figure 4 predicts that this will lead to a reduction in the HOBr reactive uptake coefficient, particularly in plumes confined to the lower troposphere, which may contribute to a slower rate of BrO cycling. For plumes in the mid–upper troposphere, γ_{HOBr} is predicted to remain high.

To date, numerical model studies of the impacts of volcanic halogens reactive halogen chemistry in the troposphere have either used a fixed uptake coefficient (Roberts et al., 2009; 2014, Kelly et al., 2013) or the termolecular approach to HOBr kinetics (Bobrowski et al., 2007; von Glasow, 2010). Figure 4 illustrates that both of these approaches will lead to modelling inaccuracies, particularly in the downwind plume. Incorporation of more realistic HOBr kinetics in these models, using the parameterisations proposed here, is recommended in order to accurately simulate the reactive bromine chemistry and plume impacts.

5 Conclusions

This study introduces a new evaluation of HOBr reactive uptake coefficients on aerosol of different compositions, in the context of the general acid-assisted mechanism. We emphasise that the termolecular kinetic approach assumed in numerical model studies of tropospheric reactive bromine chemistry to date is strictly only valid for a specific pH range. Rather, according to the general acid-assisted mechanism, the reaction kinetics for HOBr becomes independent of pH at high acidity. By re-evaluation of reported rate constant data from uptake experiments on acidified sea-salt aerosol, and consideration of relative reaction rates according to nucleophile strength, we identify that the kinetics of HOBr+Cl^-

may saturate below pH 6 to yield a second-order rate constant of $k^{II} \sim 10^4\,M\,s^{-1}$. The kinetics of HOBr+$Br^-$ saturates at $k^{II} \sim 10^8$-$10^9\,M\,s^{-1}$ at pH $< \sim 1$ based on the experimental data and kinetics estimates of Eigen and Kustin (1962) and Beckwith et al. (1996).

This study reconciles for the first time the different reported uptake reactive coefficients from laboratory experiments. The new k^{II} parameterisation yields uptake coefficients that are consistent with reported uptake experiments: $\gamma_{HOBr} = 0.6$ on supersaturated NaBr aerosol (Wachsmuth et al., 2002); $\gamma_{HOBr} > 0.2$ on HCl-acidified sea-salt aerosol (Abbatt and Wachsewsky, 1998) and $\gamma_{HOBr} = 10^{-2}$ on H_2SO_4-acidified sea-salt aerosol, with an RH dependence (Pratte and Rossi, 2006). The variation in uptake coefficient across the alkaline–aerosol transitions is similar to that previously predicted using the termolecular approach but uptake calculations using our revised kinetics of HOBr show much lower uptake coefficients for HOBr in highly acidified sea-salt aerosol, particularly for small particle radii. This is due to acid displacement of $HCl_{(g)}$ at high acidity slowing the rate of reaction of HOBr+Cl^-, thus lowering $\gamma_{HOBr+Cl}$, with dilution of $[Br^-_{(aq)}]$ at very high H_2SO_4 : sea salt ratios slowing the rate of reaction of HOBr+Br^-, thus lowering $\gamma_{HOBr+Br}$. This finding contrasts with the existing termolecular approach to uptake calculations in which the higher rate constant overcompensates for the decrease in halide concentration with increasing acidity. Thus, the termolecular approach, as currently used in numerical models of tropospheric BrO chemistry, may cause HOBr reactive uptake to be substantially overestimated in aerosol at high acidity.

Implications for BrO chemistry in the marine boundary layer have been discussed. Firstly, the HOBr uptake coefficient is predicted to be high on slightly acidified supra-micron particles but extremely low on highly acidified sub-micron particles. A first explanation for the observed Br enrichment in the sub-micron particles simultaneous to Br depletion in supra-micron particles is thereby proposed, as reactive bromine release from the supra-micron fraction may deposit and accumulate in the submicron fraction, that does not undergo significant Br^- depletion. Secondly, because the HOBr+Br^- uptake coefficient is a function of $Br^-_{(aq)}$ concentrations, a negative feedback can occur as the marine BrO chemistry evolves, and supra-micron particle $Br^-_{(aq)}$ concentrations are lowered by the release of reactive bromine. According to our revised HOBr kinetics (yielding $\gamma_{HOBr+Br-} > \gamma_{HOBr+Cl-}$), this negative feedback for $\gamma_{HOBr+Br-}$ exerts a stronger overall influence on the rate of HOBr reactive uptake than previous studies have assumed.

Calculations on volcanic aerosol show that uptake is high and accommodation limited in the concentrated near-source plume, enabling BrO formation to rapidly occur. Uptake coefficients are reduced in more dilute plumes, particularly for HOBr+Cl^-, at high temperatures (typical lower tropospheric altitudes), for small particle radii. The findings suggest that HOBr uptake on sulfate aerosol directly emitted from volcanoes can readily promote BrO cycling in plumes throughout the troposphere but that the rate of BrO cycling may be reduced by low uptake coefficients in the dispersed downwind plume, particularly at lower tropospheric altitudes. Inclusion of our revised HOBr reaction kinetics in numerical models of volcanic plume chemistry (or uptake coefficients derived therefrom) is required in order to accurately predict the impacts of volcanic halogens on the troposphere.

The Supplement related to this article is available online at doi:10.5194/acp-14-11185-2014-supplement.

Acknowledgements. T. J. Roberts and L. Jourdain are grateful for funding from LABEX VOLTAIRE (VOLatils Terre Atmosphère Interactions – Ressources et Environnement) ANR-10-LABX-100-01 (2011-20). P. T. Griffiths acknowledges the ERC for funding. We are grateful to Tony Cox and an anonymous reviewer whose comments helped to improve the manuscript.

Edited by: M. Ammann

References

Abbatt, J. P. D. and Waschewsky, G. C.G.: Heterogeneous Interactions of HOBr, HNO_3, O_3, and NO_2 with Deliquescent NaCl Aerosols at Room Temperature, J. Phys. Chem. A, 102, 3719–3725, 1998.

Ammann, M., Cox, R. A., Crowley, J. N., Jenkin, M. E., Mellouki, A., Rossi, M. J., Troe, J., and Wallington, T. J.: Evaluated kinetic and photochemical data for atmospheric chemistry: Volume VI – heterogeneous reactions with liquid substrates, Atmos. Chem. Phys., 13, 8045–8228, doi:10.5194/acp-13-8045-2013, 2013.

Barrie, L. A., Bottenheim, J. W., Schnell, R. C., Crutzen, P. J., and Rasmussen, R. A.: Ozone destruction and photochemical reactions at polar sunrise in the lower Arctic atmosphere, Nature, 334, 138–141, 1988.

Beckwith, R. C., Wang, T. X., and Margerum, D. W.: Equilibrium and Kinetics of Bromine Hydrolysis, Inorg. Chem., 35, 995–1000, 1996.

Bobrowski, N. and Platt, U.: SO_2/BrO ratios studied in five volcanic plumes, J. Volcanol. Geoth. Res., 166, 147–160, doi:10.1016/j.jvolgeores.2007.07.003, 2007.

Bobrowski, N., Honniger, G., Galle, B., and Platt, U.: Detection of bromine monoxide in a volcanic plume, Nature, 423, 273–276, doi:10.1038/nature01625, 2003.

Bobrowski, N., von Glasow, R., Aiuppa, A., Inguaggiato, S., Louban, I., Ibrahim, O. W., and Platt, U.: Reactive halogen chemistry in volcanic plumes, J. Geophys. Res., 112, D06311, doi:10.1029/2006JD007206, 2007.

Boichu, M., Oppenheimer, C., Roberts, T. J., Tsanev, V., and Kyle, P. R.: On bromine, nitrogen oxides and ozone depletion in the tropospheric plume of Erebus volcano (Antarctica), Atmos. Environ., 45, 3856–3866, 2011.

Breider, T. J., Chipperfield, M. P., Richards, N. A. D., Carslaw, K. S., Mann, G. W., and Spracklen, D. V.: Impact of BrO on dimethylsulfide in the remote marine boundary layer, Geophys. Res. Lett., 37, L02807, doi:10.1029/2009GL040868, 2010.

Carslaw, K. S., Clegg, S. L., and Brimblecombe, P.: A thermodynamic model of the system HCl-HNO_3-H_2SO_4-H_2O, including solubilities of HBr, from < 200 K to 328 K, J. Phys. Chem., 99, 11557–11574, 1995.

Clegg, S. L., Brimblecombe, P., and Wexler, A. S.: A thermodynamic model of the system H^+-NH_4^+-Na^+-SO_4^{2-}-NO_3^--Cl^--H_2O at 298.15 K, J. Phys. Chem. A, 102, 2155–2171, 1998.

Eigen, M. and Kustin, K.: The Kinetics of Halogen Hydrolysis, J. Am. Chem. Soc., 84, 1355–1361, doi:10.1021/ja00867a005, 1962.

Fickert, S., Adams, J. W., and Crowley, J. N.: Activation of Br_2 and BrCl via uptake of HOBr onto aqueous salt solutions, J. Geophys. Res., 104, 23719–23727, 1999.

Frenzel, A., Scheer, V., Sikorski, R., George, C., Behnke, W., and Zetzsch, C.: Heterogenerous Interconversion Reactions of $BrNO_2$, $ClNO_2$, Br_2, and Cl_2, J. Phys. Chem. A, 102, 1329–1337, 1998.

Gerritsen, C. M. and Margarem, D. W.: Non-Metal Redox Kinetics: Hypochlorite and Hypochlorous Acid Reactions with Cyanide, Inorg. Chem., 29, 2757–2762, 1990.

Hebestreit, K., Stutz, J., Rosen, D., Matveiv, V., Peleg, M., Luria, M., and Platt, U.: DOAS measurements of tropospheric bromine oxide in mid-latitudes, Science, 283, 55–57, 1999.

Iraci, L. T., Michelsen, R. R., Ashbourn, S. F. M., Rammer, T. A., and Golden, D. M.: Uptake of hypobromous acid (HOBr) by aqueous sulfuric acid solutions: low-temperature solubility and reaction, Atmos. Chem. Phys., 5, 1577–1587, doi:10.5194/acp-5-1577-2005, 2005.

IUPAC Task Group on Atmospheric Chemical Kinetic Data Evaluation, http://iupac.pole-ether.fr (last access: August 2014), 1999–2014.

Liu, Q. and Magarem, D. W.: Equilibrium and Kinetics of Bromine, Environ. Sci. Technol., 35, 1127–1133, 2001.

Keene, W. C., Pszenny, A. A. P., Maben, J. R., and Sander, R.: Variation of marine aerosol acidity with particle size, Geophys. Res. Lett., 29, 1101, doi:10.1029/2001GL013881, 2002.

Keene, W. C., Long, M. S., Pszenny, A. A. P., Sander, R., Maben, J. R., Wall, A. J., O'Halloran, T. L., Kerkweg, A., Fischer, E. V., and Schrems, O.: Latitudinal variation in the multiphase chemical processing of inorganic halogens and related species over the eastern North and South Atlantic Oceans, Atmos. Chem. Phys., 9, 7361–7385, doi:10.5194/acp-9-7361-2009, 2009.

Kelly, P. J., Kern, C., Roberts, T. J., Lopez, T., Werner, C., and Aiuppa, A.: Rapid chemical evolution of tropospheric volcanic emissions from Redoubt Volcano, Alaska, based on observations of ozone and halogen-containing gases, J. Volcanol. Geoth. Res., 259, 317–333, 2013.

Klassen, J. K., Hu, Z., and Williams, L. R.: Diffusion coefficients for HCl and HBr in 30 wt % to 72 wt % sulfuric acid at temperatures between 220 and 300 K, J. Geophys. Res., 103, 16197–16202, 1998.

Kumar, K. and Margarem, D. W.: Kinetics and Mechanism of General- Acid-Assisted Oxidation of Bromide by Hypochlorite and Hypochlorous Acid, Inorg. Chem., 26, 2706–2711, 1987.

Nagy, J. C., Kumar, K., and Margarem, D. W.: Non-Metal Redox Kinetics: Oxidation of Iodide by Hypochlorous Acid and by Nitrogen Trichloride Measured by the Pulsed-Accelerated-Flow Method, Inorg. Chem., 27, 2773–2780, 1988.

Parrella, J. P., Jacob, D. J., Liang, Q., Zhang, Y., Mickley, L. J., Miller, B., Evans, M. J., Yang, X., Pyle, J. A., Theys, N., and Van Roozendael, M.: Tropospheric bromine chemistry: implications for present and pre-industrial ozone and mercury, Atmos. Chem. Phys., 12, 6723–6740, doi:10.5194/acp-12-6723-2012, 2012.

Pratte, P. and Rossi, M. J.: The heterogeneous kinetics of HOBr and HOCl on acidified sea salt and model aerosol at 40–90 % relative humidity and ambient temperature, Phys. Chem. Chem. Phys., 8, 3988–4001, 2006.

Read, K. A., Mahajan, A. S., Carpenter, L. J., Evans, M. J., Faria, B. V. E., Heard, D. E., Hopkins, J. R., Lee, L. D., Moller, S. J., Lewis, A. C., Mendes, L., McQuaid, J. B., Oetjen, H., Saiz-Lopez, A., Pilling, M. J., and Plane, J. M. C.: Extensive halogen-mediated ozone destruction over the tropical Atlantic Ocean, Nature, 453, 1232–1235, doi:10.1038/nature07035, 2008.

Roberts, T. J., Braban, C. F., Martin, R. S., Oppenheimer, C., Adams, J. W., Cox, R. A., Jones, R. L., and Griffiths, P. T, Modelling reactive halogen formation and ozone depletion in volcanic plumes, Chem. Geol., 263, 151–163, 2009.

Roberts, T. J., Martin, R. S., and Jourdain, L.: Reactive bromine chemistry in Mount Etna's volcanic plume: the influence of total Br, high-temperature processing, aerosol loading and plume-air mixing, Atmos. Chem. Phys., 14, 11201–11219, doi:10.5194/acp-14-11201-2014, 2014.

Saiz-Lopez, A. and von Glaosw, R.: Reactive halogen chemistry in the troposphere, Chem. Soc. Rev., 41, 6448–6472, 2012.

Sander, R.: Compilation of Henry's Law Constants for Inorganic and Organic Species of Potential Importance in Environmental Chemistry (Version 3), http://www.henrys-law.org (last access: November 2013), 1999.

Sander, R., Keene, W. C., Pszenny, A. A. P., Arimoto, R., Ayers, G. P., Baboukas, E., Cainey, J. M., Crutzen, P. J., Duce, R. A., Hönninger, G., Huebert, B. J., Maenhaut, W., Mihalopoulos, N., Turekian, V. C., and Van Dingenen, R.: Inorganic bromine in the marine boundary layer: a critical review, Atmos. Chem. Phys., 3, 1301–1336, doi:10.5194/acp-3-1301-2003, 2003.

Sander, R., Baumgaertner, A., Gromov, S., Harder, H., Jöckel, P., Kerkweg, A., Kubistin, D., Regelin, E., Riede, H., Sandu, A., Taraborrelli, D., Tost, H., and Xie, Z.-Q.: The atmospheric chemistry box model CAABA/MECCA-3.0, Geosci. Model Dev., 4, 373–380, doi:10.5194/gmd-4-373-2011, 2011.

Smoydzin, L. and von Glasow, R.: Do organic surface films on sea salt aerosols influence atmospheric chemistry? – a model study, Atmos. Chem. Phys., 7, 5555–5567, doi:10.5194/acp-7-5555-2007, 2007.

Schroeder, W. H., Anlauf, K. G., Barrie, L. A., Lu, J. Y., Steffen, A., Schneeberger, D. R., and Berg, T.: Arctic springtime depletion of mercury, Nature, 394, 331–332, doi:10.1038/28530, 1998.

Seinfeld, J. H. and Pandis, S. N.: Atmospheric Chemistry and Physics – From Air Pollution to Climate Change, John Wiley & Sons, p. 440, 1998.

Simpson, W. R., von Glasow, R., Riedel, K., Anderson, P., Ariya, P., Bottenheim, J., Burrows, J., Carpenter, L. J., Frieß, U., Goodsite, M. E., Heard, D., Hutterli, M., Jacobi, H.-W., Kaleschke, L., Neff, B., Plane, J., Platt, U., Richter, A., Roscoe, H., Sander,

R., Shepson, P., Sodeau, J., Steffen, A., Wagner, T., and Wolff, E.: Halogens and their role in polar boundary-layer ozone depletion, Atmos. Chem. Phys., 7, 4375–4418, doi:10.5194/acp-7-4375-2007, 2007.

Vogt, R., Crutzen, P. J., and Sander, R.: A mechanism for halogen release from sea-salt aerosol in the remote marine boundary layer, Nature, 383, 327–330, 1996.

von Glasow, R.: Atmospheric Chemistry in Volcanic Plumes, P. Natl. Acad. Sci. USA, 107, 6594–6599, 2010.

von Glasow, R., Sander, R., Bott, A., and Crutzen, P. J.: Modeling halogen chemistry in the marine boundary layer 1. Cloud-free MBL, J. Geophy. Res., 107, 4341, doi:10.1029/2001JD000942, 2002.

von Glasow, R., von Kuhlmann, R., Lawrence, M. G., Platt, U., and Crutzen, P. J.: Impact of reactive bromine chemistry in the troposphere, Atmos. Chem. Phys., 4, 2481–2497, doi:10.5194/acp-4-2481-2004, 2004.

Wachsmuth, M., Gäggeler, H. W., von Glasow, R., and Ammann, M.: Accommodation coefficient of HOBr on deliquescent sodium bromide aerosol particles, Atmos. Chem. Phys., 2, 121–131, doi:10.5194/acp-2-121-2002, 2002.

Wang, T. X. and Margarem, D. W.: Kinetics of Reversible Chlorine Hydrolysis: Temperature Dependence and General-Acid/ Base-Assisted Mechanisms, Inorg. Chem., 33, 1050–1055, 1994.

Wang, T. X., Kelley, M. D., Cooper, J. N., Beckwith, R. C., and Margerum, D. W.: Equilibrium, kinetic, and UV-spectral characteristics of aqueous bromine chloride, bromine, and chlorine species, Inorg. Chem., 33, 5872–5878, 1994.

Wexler, A. S. and Clegg, S. L.: Atmospheric aerosol models for systems including the ions H^+, NH_4^+, Na^+, SO_4^{2-}, NO_3^-, Cl^-, Br^- and H_2O, J. Geophys. Res., 107, 4207–4220, 2002.

Wilson, T. R. S.: Salinity and the major elements of sea water, in: Chemical Oceanography, 1, 2 Edn., edited by: Riley, J. P. and Skirrow, G., Academic, Orlando FL, 365–413, 1975.

Yang, X., Cox, R. A., Warwick, N. J., Pyle, J. A., Carver, G. D., O'Connor, F. M., and Savage, N. H.: Tropospheric bromine chemistry and its impacts on ozone: A model study, J. Geophys. Res., 110, D23311, doi:10.1029/2005JD006244, 2005.